Chinese Chemical Letters 36 (2025) 110724

Contents lists available at ScienceDirect

Chinese Chemical Letters

journal homepage: www.elsevier.com/locate/cclet

Significantly boosting circularly polarized luminescence by synergy of helical and planar chirality

Fengying Ye[a], Ming Hu[a], Jun Luo[b], Wei Yu[a], Zhirong Xu[a], Jinjin Fu[a], Yansong Zheng[a,*]

[a] Key Laboratory of Material Chemistry for Energy Conversion and Storage, Ministry of Education, School of Chemistry and Chemical Engineering, Huazhong University of Science and Technology, Wuhan 430074, China
[b] Tongji School of Pharmacy, Huazhong University of Science and Technology, Wuhan 430030, China

ARTICLE INFO

Article history:
Received 9 October 2024
Revised 3 December 2024
Accepted 4 December 2024
Available online 5 December 2024

Keywords:
Synergy of helical and planar chirality
Tetraphenylethylene helicate
Boosting circularly-polarized luminescence
Helical nanofibers
Self-assembly

ABSTRACT

To get large dissymmetric factor (g_{lum}) of organic circularly polarized luminescence (CPL) materials is still a great challenge. Although helical chirality and planar chirality are usual efficient access to enhancement of CPL, they are not combined together to boost CPL. Here, a new tetraphenylethylene (TPE) tetracycle acid helicate bearing both helical chirality and planar chirality was designed and synthesized. Uniquely, synergy of the helical chirality and planar chirality was used to boost CPL signals both in solution and in helical self-assemblies. In the presence of octadecylamine, the TPE helicate could form helical nanofibers that emitted strong CPL signals with an absolute g_{lum} value up to 0.237. Exceptionally, followed by addition of *para*-phenylenediamine, the g_{lum} value was successively increased to 0.387 due to formation of bigger helical nanofibers. Compared with that of TPE helicate itself, the CPL signal of the self-assemblies was not only magnified by 104-fold but also inversed, which was very rare result for CPL-active materials. Surprisingly, the interaction of TPE helicate with xylylenediamine even gave a gel, which was transformed into suspension by shaking. Unexpectedly, the suspension showed 40-fold stronger CPL signals than the gel with signal direction inversion each other. Using synergy of the helical chirality and planar chirality to significantly boost CPL intensity provides a new strategy in preparation of organic CPL materials having very large g_{lum} value.

The circularly polarized luminescence (CPL) materials have important potential applications in 3D display [1], information storage and processing [2,3], molecule switches [4], biological probe and tag [5,6], chiral sensors [7], and so on [8,9]. However, the key index dissymmetric factor (g_{lum}) of the CPL materials is still low and seriously limits their practical application.

One of the most efficient methods for producing and improving the CPL property is to construct helical chirality or supramolecular helical chirality of the luminescent molecules. For example, helicenes have been extensively studied as CPL materials [10–12]. Other luminescent molecules with helical chirality such as cyclic alkyl amino carbene derived propeller [13], tri(2,4,6-trichlorophenyl)methyl radical derivatives [14], boron heptaaryldipyrromethene [15], perylene diimide dimer with double π-helix [16], helical metal complexes [17,18], and helical polymers [19–21], all display strong CPL emission. Besides the molecular chirality, by forming ordered supramolecular helical aggregates or helical arrangement of luminophores, the CPL property could be substantially boosted and improved [22,23]. For instance, pyrene bearing chiral amino acid substitute did not emit CPL signal in solution while the assembled nanofibers show strong CPL emission [24]. Two pyrenes connected with chiral cyclohexanediamine could pack into hexagonal superhelix, and amplified CPL signals by 53-fold to give an absolute g_{lum} of up to 0.0265 [25]. Achiral luminophores were confined in helical nanotube also aroused strong CPL, and the g_{lum} was even got to 0.1 [26]. These examples demonstrate that the helical structure and helical assembly are important strategy for boosting CPL signals.

In addition, molecular planar chirality is also important access to obtain CPL signals of luminescent molecules [27–34]. The luminophores bearing planar chirality are generally macrocyclic derivatives such as paracyclophanes [27] and pillararenes [28], and possess large rigidity. Therefore, they usually show strong and stable CPL emission, and can display CPEL [30,31]. The absolute g_{lum} values of them are generally at 10^{-3} level and few of them can get 10^{-2} level [32,33]. By upconvesion emission and doping in liquid crystal, planar chiral biphenylparacyclophane even can get a g_{lum} value up to 0.19 and could be used in asymmetric polymerization

* Corresponding author.
E-mail address: zyansong@hotmail.com (Y. Zheng).

https://doi.org/10.1016/j.cclet.2024.110724
1001-8417/

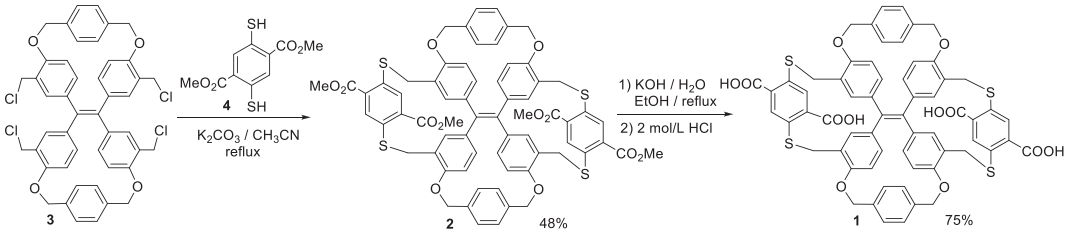

Fig. 1. Synthetic route of TPE tetracycle tetracid **1**.

[34], showing potential of planar chirality in developing CPL materials. Although these significant progresses have been made, the report about CPL material with excellent property, especially with high g_{lum} value, is still rare. By combining planar and helical chirality in one luminophore to boost CPL signals is not reported up to now.

Since CPL materials are usually used in solid state, aggregation-induced emission (AIE) molecules have inherent advantage because of their stronger emission in solid state [19,22,23,35,36]. Tetraphenylethylene (TPE) and their derivatives are typical AIE compounds and extensively studied as solid emitters. Therefore, chiral TPE derivatives are also investigated as CPL materials, but their chirality is often obtained by introduction of external chiral groups. The inherent helical chirality of TPE propeller-like conformation is not adequately exploited [37–44]. Here, new TPEtetracid helical enantiomers bearing both helical chirality and planar chirality were synthesized. It was found that the synergies of the helical chirality and planar chirality could be uniquely beneficial for significantly magnifying CPL signals both in solution and in helical self-assembles, giving a very high g_{lum} value up to 0.386.

The TPE tetracycle tetracid helicate **1** was synthesized according to the previous synthetic route (Fig. 1) [37,38]. TPE tetracycle tetraester **2** was easily obtained through intramolecular nucleophilic substitution of dichloromethyl TPEdicycle **3** by *p*-dithiol-*p*-bimethylterephthalate in 48% yield. Then, the hydrolysis of tetraester **2** by potassium hydroxide in a mixed solvent of water and ethanol furnished the target molecule TPE tetracycle tetracid **1**. The structures of **1** and **2** were fully characterized by NMR, MS and IR spectra (Figs. S1-S20 in Supporting information).

Unexpectedly, while the starting compound **3** emitted strong fluorescence both in solution and in solid, TPE tetracycle tetracid compounds **1** and **2** were almost non-emissive in both solution and solid. In DMSO, DMSO/H_2O 5:95 suspension, and solid, the fluorescence quantum yield (Φ_f) of **1** was only 0.03%, 0.98% and 0.11%, respectively. Similarly, TPE tetracycle tetraester **2** was also emissionless in solution and solid. However, when NaOH was added into the solution of **1** in DMSO, the fluorescence intensity was gradually increased (Fig. S29A in Supporting information). At 4 equiv. NaOH, the Φ_f was 66%, which was 2200-fold larger than that of **1** in DMSO, indicating that it could be used as fluorescent probe for basicity detection (Fig. S21 and Table S1 in Supporting information). From this result, the emissionless property of **2** and **1** should be ascribed to the electron-withdrawing carboxyl groups, leading to fluorescence quenching through intramolecular photoinduced electron transfer from electron-rich TPE unit to electron-withdrawing terephthalate ring. In the presence of sodium hydroxide, terephthalic acid was transformed into less electron-withdrawing terephythalate anion so that the fluorescence was increased.

In the presence of organic amines, including *n*-hexylamine (HA), *n*-dodecylamine (DA), *n*-octadecylamine (OA), benzylamine (BA), *o*-phenylenediamine (*o*PA), *m*-phenylenediamine (*m*PA), *p*-phenylenediamine (*p*PA), ethylenediamine (EDA), 1,4-butanediamine (BDA), 1,6-hexanediamine (HAD), *trans*-1,4-cyclohexanediamine (CDA), 1,4-xylylenediamine (XDA), TPE tetracycle acid **1** generally became fluorescent from emissionless. Due to stronger basicity, alkyl amine aroused much stronger fluorescence of **1** than the aromatic amines. Especially, OA, BDA, CDA, and XDA could give rise to the strongest emission (Figs. S29B and C in Supporting information). Besides, it was noted that OA, BDA, HDA, and XDA led to blue color of fluorescence while other amines furnished emission with green color. From absorption spectrum, the mixture of **1** with amines having blue fluorescence showed blue shift compared with the amines arousing green fluorescence. It seemed that the emission had shorter wavelength as alkyl groups became larger, such as from HA, DA to OA, or from EDA, BDA to HAD (Fig. S29D in Supporting information). By binding larger alkyl groups, the phenyl rings of the TPE unit would have larger repulsive force, leading to less conjugation and blue-shift emission and absorption.

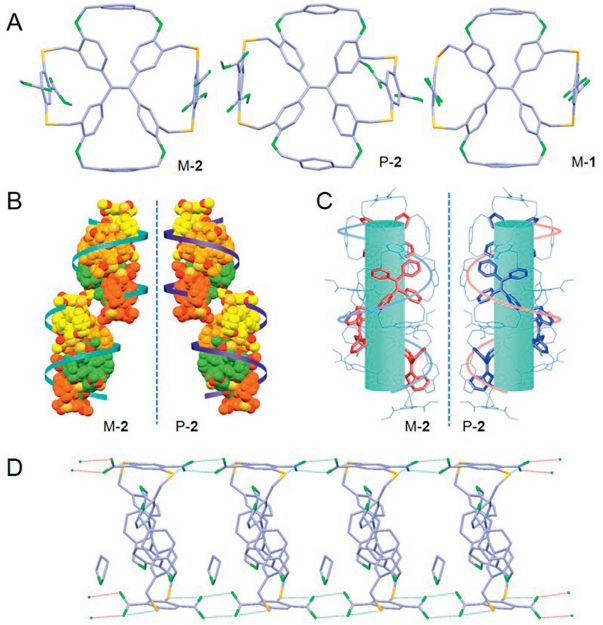

Fig. 2. (A) Crystal structures of M-**2**, P-**2** and M-**1**. Molecular packing of M-**2** and P-**2** in spacefill type (B) and in wireframe and stick type (C) in a crystal cell. (D) Packing of M-**1** in crystal state. The dotted line denoted hydrogen bonds. The hydrogen atoms and solvent molecules in A, B and C were removed for clarity.

Due to immobilization of the propeller-like conformation, TPE tetracycle tetraester **2** was easily resolved into two stable single helical enantiomers by chiral HPLC using CHIRALPAK IE column. Fortunately, the crystal structures of racemic **2** and its two enantiomers were obtained. While both left-handed helical (M) isomer and right-handed helical (P) isomer were found in the single crystal of racemic **2** in equal numbers, only single-handed helical isomer existed in the enantiomer crystal (Figs. 2A-C). The crystal structure of these two enantiomers showed that the first peak in HPLC was M-isomer and the second peak was P-isomer. It was

noted that there was planar chirality of the terephthalate units in addition to the helical chirality. For M-**2**, the planar chirality of the two terephthalate units was S-configuration while the planar chirality of P-**2** was R-one. The hydrolyzed product M-**1** of M-**2** also gave the same planar chirality. The helical chirality determined the direction of the planar chirality of the two terephthalate units. For simplicity, the planar chirality symbol in the enantiomers names was omitted.

By intermolecular interactions of CH_3-π, CH_3-O=C, ArH-O=C, and so on, the methyl ester groups of one molecule of **2**, could insert into the macrocyclic cavity of another molecule, and packed into column structure from vertical direction to the molecular surface in a crystal cell. However, the packing molecules in one column structure were not parallel each other but were tilted each other. Therefore, the molecules of M-**2** made a right-handed helical tilted arrange while P-**2** gave a left-handed tilted overlapping (Fig. 2B). By viewing from the pointing direction of methyl ester groups that had interactions with other molecules, it could be found that the methyl ester groups of M-**2** molecules were around one axle in a right-handed helical direction and those of P-**2** molecules surrounded the axle in a left-handed helical direction (Fig. 2C). Unexpectedly, the chirality of the resultant helical column was inverse to the chirality of molecule.

In contrast, the molecules of racemic **2** were all parallel one another and no supramolecular chirality appeared (Fig. 2D). For the acid M-**1**, molecules could also pack into column structures by strong intermolecular hydrogen bonds between carboxylic groups, but they were parallel each other. Noticeably, between two pairs of hydrogen bonds there was a big space, which included one molecule of THF, just like hydrogen-bonded organic frameworks (HOF) structure.

The two enantiomers of TPE tetracycle ester M-**2** and P-**2** and TPE tetracycle tetracid M-**1** and P-**1** showed strong Cotton effect and mirror symmetrical CD spectra in THF. However, due to almost no-emission, no CPL signal was observed (Figs. S22 and S23 in Supporting information). After addition of NaOH, the two enantiomers of **1** not only showed CD signals but also strong CPL signals at 520 nm in DMSO (Fig. S30 in Supporting information). The CD spectra had obvious bisignate bands, indicating the helical structure of **1** because of the exciton coupling of neighboring four phenyl rings. When 2 equiv. NaOH was added, the CPL g_{lum} was 3.5×10^{-3} for M-**1** and -3.60×10^{-3} for P-**1**. As more NaOH was added, the fluorescence was stronger and CD signals were also increased, but CPL signals and g_{lum} value was not further increased except the CPL curves became more stable and smoother. This result demonstrated that the CPL signals had not linear correlation with fluorescence intensity. Moreover, the g_{lum} value was increased by 1.7 times compared with the corresponding TPE tetracycle without carboxylic groups (Fig. S24 in Supporting information) [37], suggesting that the planar chirality in one helical molecule was helpful for boosting CPL signals

Subsequently, organic bases modified with long alkyl chains were employed to generate fluorescence and facilitate the self-assembly of molecules. It is well-known that a system with strong fluorescence emission is one of the sufficient conditions to ensure strong CPL emission. Three bases with strong fluorescence emission were selected: OA, DA, and XA. When hydrocarbyl monoamines with different length such as BA, HA, DA, and OA were tested, enantiomers of **1** displayed strong chiroptical property. Among these tested organic bases, OA gave rise to the strongest CPL signals (Fig. 3). In the presence of 2 equiv. OA, the Cotton effect in the CD spectrum of M-**1** and P-**1** was mirror symmetrical and showed bisignate band. However, the signal direction was opposite to that of the TPE tetracycle enantiomers themselves. Exceptionally, a very strong CPL signals up to 1600 mdeg was observed. The resultant g_{lum} value was −0.237 for M-**1** and +0.237 for P-**1** at 460 nm. Compared with NaOH, the addition of OA made the CPL signals be magnified by 64-fold but the direction of the CPL direction was inverse. The CPL signal from the mixture of **1** and OA was also 1.3-fold stronger than that of acid-base system from TPE tetracycle without planar chirality [38], corroborating that the additional planar chirality was beneficial to CPL boosting. At molar ratio of OA/**1** 4:1, the CPL decreased a little but still had absolute g_{lum} value up to 0.18. Meanwhile, Φ_f was increased from 3.0% to 10%. Therefore, the synergy of helical and planar chirality would be profitable to boost CPL signals not only for chiral luminophore itself but also for its chiral self-assembles. To our knowledge, this is the first example for using the combination of helical and planar chirality to enhance CPL emission.

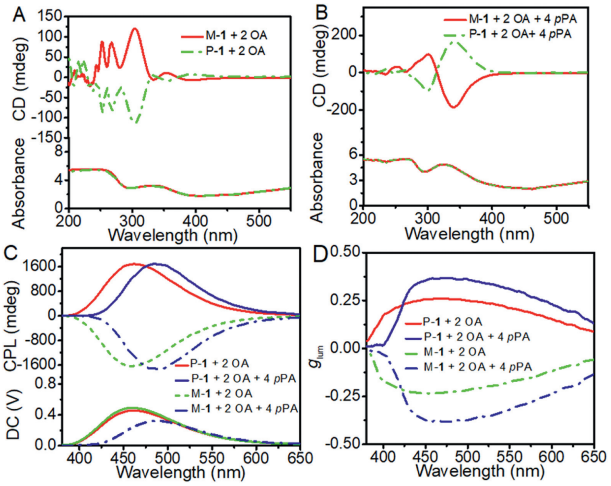

Fig. 3. CD and absorption spectra of M-**1** and P-**1** with (A) 2 equiv. OA, (B) 2 equiv. OA and 4 equiv. *p*PA. (C) CPL spectra of OA/**1** 2:1 without and with further added 4 equiv. *p*PA. (D) The change of g_{lum} with the emission wavelength. [M-**1**] = [P-**1**] = 1/2 [OA] = 1/4 [*p*PA] = 1.0×10^{-3} mol/L in THF. λ_{ex} = 350 nm.

Very interestingly, when other various amines, such as XA, HDA, *p*PA, were added to the **1**+OA system, only 4 equiv. *p*PA was able to enhance the CD and CPL signals of the system (Figs. 3C and D). The Cotton effect was magnified from 10 mdeg to 170 mdeg at 350 nm and showed a conspicuous bisignate band between 500 nm and 266 nm, hinting that the addition of *p*PA changed the assembly pattern. It was also noticed that the solution of OA/**1** 2:1 mixture in THF was changed from suspension to sticky state after 4 equiv. *p*PA was added. The CPL g_{lum} values were magnified from −0.237 and +0.237 to −0.386 and +0.386 for M-**1** and P-**1** at 490 nm, respectively, giving a 1.6-fold enhancement while the CPL direction was kept to be the same compared with the OA/**1** 2:1 mixture without *p*PA. By comparing the **1**/NaOH system, the CPL signals was boosted by 107-fold.

Due to the long alkyl structure of OA, the solution of OA/**1** 2:1 in THF formed good transparent film on the quartz glass surface. A strong CPL signals was observed and had a g_{lum} value of −0.230 and +0.234 for M-**1** and for P-**1** at 427 nm in film, respectively, showing the same CPL direction and similar CPL intensity as that in suspension (Fig. S25 in Supporting information).

Surprisingly, by interaction with 2 equiv. XDA, both M-**1** and P-**1** could form a gel in DMSO when the concentration was increased to 2.0×10^{-3} mol/L. By shaking, the gel could be transformed into a suspension (Fig. S31 in Supporting information). Notably, the suspension showed stronger blue fluorescence than the gel, with a Φ_f of 36% and 7.3%, respectively (Fig. S26 in Supporting information).

Meanwhile, the gels of M-**1** and P-**1** with XDA displayed strong mirror symmetrical CD signals and had obvious multiple bisignate bands between 250 nm and 400 nm, indicating the helical chirality of TPE unit. In addition, M-**1** aroused positive Cotton effect and P-**1**

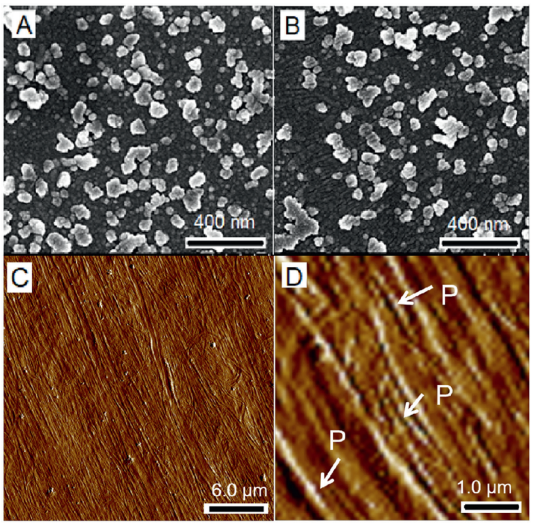

Fig. 4. SEM images of M-**1** (A) and P-**1** (B). (C, D) AFM images of M-**1** with 2 equiv. OA in THF.

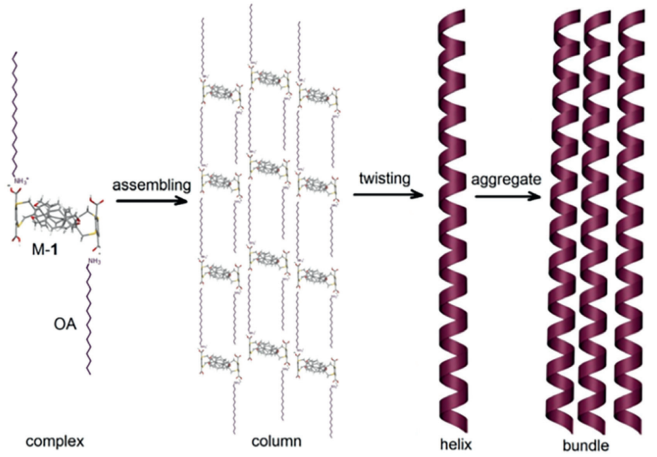

Fig. 5. Mechanism of the nano-helices formation.

led to negative one, which was in accordance with that of themselves or after interaction with NaOH (Fig. S32A in Supporting information). Unexpectedly, the suspension of M-**1** and P-**1** with XDA showed much stronger Cotton effect and even inverse CD signals compared with the gel (Fig. S32B in Supporting information). The direction of the CD signals was the same as that of the suspension of M-**1** and P-**1** with OA.

Moreover, the suspension also exhibited much stronger CPL signals than the gel, accompanying with opposite direction (Figs. S32C and D in Supporting information). At 460 nm, the CPL g_{lum} value was up to -6.18×10^{-2} and 6.73×10^{-2} for M-**1** and P-**1** in suspension, respectively, while the g_{lum} value of M-**1** and P-**1** in gel was 1.76×10^{-3} and -1.64×10^{-3}, respectively. By change from gel to suspension, not only the CPL signal was amplified by 40-fold but also the CPL direction was reversed.

Field emission scanning electron microscopy (FE-SEM) disclosed that the solution of pure enantiomers M-**1** and P-**1** in THF formed nano-particles with diameter distribution from 20 nm to 100 nm (Figs. 4A and B). By addition of 4 equiv. NaOH, the mixture also had morphology of nanoparticles with almost the same size distribution as the enantiomers themselves (Fig. S27 in Supporting information). In a sharp contrast, after OA was added, the resultant suspension was composed of nano-helices with very large aspect. The nano-helix had a very uniform diameter of about 90 nm but their length was larger than 40 μm. As a result, the long nano-helices easily aggregated into bundles with a diameter of 700 nm to 3000 nm, which were made up of 60 nano-helices to 1100 nano-helices (Figs. 4C and D). Moreover, the nano-helix had a right-handed helical chirality, which was contrary to that of M-**1** molecule. This should be the reason why pure TPE tetracycle enantiomers and their mixture helical fibers exhibited CD and CPL signals with the opposite direction. When *p*PA was added in the mixture of M-**1**/OA, the morphology was still long helical nano-fibers. However, the bundles formed by aggregation of nano-helices became larger and had a diameter of up to 4500 nm (Fig. S28 in Supporting information).

The gel and solution of the TPE tetracycle enantiomers with XDA in DMSO was also measured for their morphology by SEM and AFM. Unexpectedly, the gel was composed of nanoparticles that aggregated into blocks that enabled gelation of the solvent (Fig. S33A in Supporting information). This result was very different from most of gels that were composed of nanofibers. However, by shaking the gel, the resultant suspension was disclosed to be nanofibers having 16 μm long and 30-50 nm wide (Fig. S33B in Supporting information). Intriguingly, AFM images revealed that the nanofibers of M-**1**/XDA mixture were right-handed helical while those of P-**1**/XDA mixture had left-handed helical structure (Figs. S33C and D in Supporting information). The helical direction of the nanofibers was inverse to that of the enantiomers themselves, arousing the reversed CD and CPL signals of the suspension. With comparison, due to no formation of supramolecular helical structure, the gel and the mixture of enantiomers/NaOH showed the chiroptical signals with the same direction as the helical direction of the enantiomers themselves but small absolute g_{lum} value.

From the observation above, the formation mechanism of the nano-helices and micro-bundles was proposed as the following (Fig. 5). After 2 equiv. OA was added, the tetracid M-**1** formed 1:2 complex of M-**1**/2OA. Then the complexes could form column structure by intermolecular van der Waals force, CH_3-π and CH-π interactions, and so on, just like the crystal packing of **2**. Due to helical chirality of TPE unit, the formed column structure by the M-**1**/2OA complexes tended to twist toward right-handed direction to form P-helix, which was similar to the P-packing of molecules of M-**2** in crystal structure. Finally, due to very large aspect ratio of the helices, they aggregated into bundles by van der Waals force between long alkyl chains, Coulombic attraction between ions, and so on. After addition of *p*PA, due to further acid-base interaction with the remained carboxylic acid groups, more nano-helices aggregated to form larger bundles. The formation of helical fiber and its enlargement should be the main reason why the CPL was boosted after sequential addition of OA followed by *p*PA.

Due to bearing two amino groups, when DXA was mixed with **1** in DMSO, the acid-base interaction was so fast that the formed salt aggregated into nanoparticles and grew into disordered massive block structure. Therefore, the CD and CPL signals of the gel were not large and had the same helical direction with gelator molecule itself. After the gel was shaken, the **1**/DXA mixture could assemble into ordered column just like that in Fig. 5 by direct connection of one molecule of DXA with two molecules of **1**. The column twisted into helices that aggregated into bigger helical nanofibers, realizing the magnification of chiroptical signals and helical direction inversion.

In conclusion, a new TPE tetracycle acid helicate **1** with both helical chirality and planar chirality was synthesized. This TPE tetracycle acid was emissionless but became strong fluorescence after it reacted with base. Upon interaction with NaOH, its enantiomer showed strong CPL signal, which was 1.7-fold larger than that of TPE tetracycle without planar chirality. In the presence of 2 equiv. OA, the CPL signals was magnified by 64-fold and had abso-

lute g_{lum} up to 0.237 due to formation of nano-helices. Compared with CPL system without planar chirality, the CPL signal was also enhanced. Exceptionally, after further addition of *p*PA that could arouse larger bundles of the nano-helices, the absolute CPL g_{lum} value was magnified from 0.237 to 0.386. In addition, by the interaction of the TPE enantiomers with diamine XDA, a gel was obtained in DMSO. By shaking, the gel was transformed into suspension that could boost the CPL signal through change of the disordered massive blocks into helical nanofibers. Interestingly, by formation of nanofibers not only the CPL signals were boosted but also the CPL direction could be reversed. Uniquely, the enhancement and magnification of CPL signals was implemented by synergy of the helical chirality and planar chirality both in solution and in self-assemblies. This result provided a new strategy in preparation of CPL materials having very high dissymmetric factor.

Declaration of competing interest

The authors declare that they have no known competing financial interests or personal relationships that could have appeared to influence the work reported in this paper.

CRediT authorship contribution statement

Fengying Ye: Writing – original draft, Investigation, Funding acquisition, Formal analysis, Data curation. **Ming Hu:** Funding acquisition, Formal analysis, Data curation. **Jun Luo:** Writing – review & editing, Methodology. **Wei Yu:** Investigation, Data curation. **Zhirong Xu:** Investigation, Data curation. **Jinjin Fu:** Investigation, Data curation. **Yansong Zheng:** Writing – review & editing, Writing – original draft, Visualization, Validation, Supervision, Project administration, Methodology, Investigation, Funding acquisition, Formal analysis, Data curation, Conceptualization.

Acknowledgments

The authors thank National Natural Science Foundation of China (Nos. 22072050, 22372066 and 22301090), the Open Research Fund (No. 2024JYBKF05) of Key Laboratory of Material Chemistry for Energy Conversion and Storage (HUST) Ministry of Education, and the China Postdoctoral Science Foundation (No. 2023M731189) for financial support, and thank the Analytical and Testing Centre at Huazhong University of Science and Technology for measurement.

Supplementary materials

Supplementary material associated with this article can be found, in the online version, at doi:10.1016/j.cclet.2024.110724.

References

[1] S.H. Chen, D. Katsis, A.W. Schmid, et al., Nature 397 (1999) 506–508.
[2] C. Wagenknecht, C.M. Li, A. Reingruber, et al., Nat. Photonics 4 (2010) 549–552.
[3] J.F. Sherson, H. Krauter, R.K. Olsson, et al., Nature 443 (2006) 557–560.
[4] B.L. Feringa, Acc. Chem. Res. 34 (2001) 504–513.
[5] J. Yuasa, T. Ohno, H. Tsumatori, et al., Chem. Commun. 49 (2013) 4604–4606.
[6] R. Carr, N.H. Evans, D. Parker, Chem. Soc. Rev. 41 (2012) 7673–7686.
[7] F. Song, G. Wei, X. Jiang, et al., Chem. Commun. 49 (2013) 5772–5774.
[8] S. Du, Y. Wang, M. Liu, et al., Chin. Chem. Lett. 35 (2024) 109256.
[9] S. Jiang, H. Guo, F. Yang, et al., Chin. Chem. Lett. 33 (2022) 2442–2446.
[10] X. Wang, X. Cheng, W. Zhang, et al., Chin. Chem. Lett. 36 (2025) 110047.
[11] J.K. Li, X.Y. Chen, Y.L. Guo, et al., J. Am. Chem. Soc. 143 (2021) 17958–17963.
[12] X. Wu, J.W. Huang, B.K. Su, et al., Adv. Mater. 34 (2022) 2105080.
[13] J. Lorkowski, D. Bouetard, P. Yorkgitis, et al., Angew. Chem. Int. Ed. 62 (2023) e202305404.
[14] P.M. Burrezo, V.G. Jiménez, D. Blasi, et al., Angew. Chem. Int. Ed. 58 (2019) 16282.
[15] M. Toyoda, Y. Imai, T. Mori, J. Phys. Chem. Lett. 8 (2017) 42.
[16] Y. Liu, Z. Ma, Z. Wang, et al., J. Am. Chem. Soc. 144 (2022) 11397–11404.
[17] M. Louis, Y.B. Tan, P. Reine, et al., ACS Omega 8 (2023) 5722–5730.
[18] L. Wang, Z. Yao, W. Huang, et al., Inorg. Chem. Front. 10 (2023) 3664–3674.
[19] K.R. Zhang, M. Hu, Y.S. Zheng, et al., Chin. Chem. Lett. 33 (2022) 1505–1510.
[20] H. Zhong, B. Zhao, J. Deng, Adv. Optical Mater. 11 (2023) 2202787.
[21] S. Yang, S. Zhang, F. Hu, et al., Coord. Chem. Rev. 485 (2023) 215116.
[22] Y. Sang, J. Han, T. Zhao, Adv. Mater. 32 (2019) 1900110.
[23] H. Li, B.S. Li, B.Z. Tang, Chem. Asian J. 14 (2019) 674688.
[24] Z. Wang, A. Hao, P. Xing, Angew. Chem. Int. Ed. 59 (2020) 11556–11565.
[25] S. Hu, L. Hu, X. Zhu, et al., Angew. Chem. Int. Ed. 60 (2021) 19451–19457.
[26] J. Liang, P. Guo, X. Qin, et al., ACS Nano 14 (2020) 3190–3198.
[27] J.F. Chen, Q.X. Gao, H. Yao, et al., Chem. Commun. 60 (2024) 6728–6740.
[28] K. Wada, T. Ogoshi, Mater. Chem. Front. 8 (2024) 1212–1229.
[29] C. Ge, W. Shang, Z. Chen, et al., Angew. Chem. Int. Ed. 63 (2024) e202408056.
[30] X.J. Liao, D. Pu, L. Yuan, et al., Angew. Chem. Int. Ed. 62 (2023) e202217045.
[31] D.W. Zhang, J.M. Teng, Y.F. Wang, et al., Mater. Horiz. 8 (2021) 3417–3423.
[32] K. Matsumura, R. Inoue, Y. Morisaki, Adv. Funct. Mater. 34 (2024) 2310566.
[33] M. Hasegawa, W. Xiao, Y. Ishida, et al., Adv. Funct. Mater. 34 (2024) 2315215.
[34] D. Han, X. Yang, J. Han, Nat. Commun. 11 (2020) 5659.
[35] M. Hu, H.T. Feng, Y.X. Yuan, Coord. Chem. Rev. 416 (2020) 213329.
[36] A. Nitti, D. Pasini, Adv. Mater. 32 (2020) 1908021.
[37] J.B. Xiong, H.T. Feng, J.P. Sun, J. Am. Chem. Soc. 138 (2016) 11469–11472.
[38] Y.X. Yuan, M. Hu, K.R. Zhang, Mater. Horiz. 7 (2020) 3209–3216.
[39] M. Hu, F.Y. Ye, C. Du, Angew. Chem. Int. Ed. 61 (2021) e202115216.
[40] F.Y. Ye, M. Hu, C. Du, Adv. Opt. Mater. 11 (2023) 2201784.
[41] F.Y. Ye, M. Hu, Y.S. Zheng, ACS Appl. Mater. Interfaces 15 (2023) 42056–42065.
[42] H. Qu, Y. Wang, Z. Li, et al., J. Am. Chem. Soc. 139 (2017) 18142–18145.
[43] Q. Meng, L. Cui, Q. Liao, et al., Chem. Commun. 58 (2022) 10384–10387.
[44] M. Hu, F.Y. Ye, C. Du, et al., ACS Nano 15 (2021) 16673–16682.